Accepted Manuscript

Title: Platinum catalysed aerobic selective oxidation of cinnamaldehyde to cinnamic acid

Authors: Lee J. Durndell, Costanza Cucuzzella, Christopher M.A. Parlett, Mark A. Isaacs, Karen Wilson, Adam F. Lee

PII: S0920-5861(18)30145-7
DOI: https://doi.org/10.1016/j.cattod.2018.02.052
Reference: CATTOD 11277

To appear in: *Catalysis Today*

Received date: 29-11-2017
Revised date: 22-2-2018
Accepted date: 27-2-2018

Please cite this article as: Lee J.Durndell, Costanza Cucuzzella, Christopher M.A.Parlett, Mark A.Isaacs, Karen Wilson, Adam F.Lee, Platinum catalysed aerobic selective oxidation of cinnamaldehyde to cinnamic acid, Catalysis Today https://doi.org/10.1016/j.cattod.2018.02.052

Platinum catalysed aerobic selective oxidation of cinnamaldehyde to cinnamic acid

Lee J. Durndell,[a] Costanza Cucuzzella,[a] Christopher M. A. Parlett,[a] Mark A. Isaacs,[a] Karen Wilson[b] and Adam. F. Lee[b*]

[a]European Bioenergy Research Institute, Aston University, Birmingham, B4 7ET, UK

[b]School of Science, RMIT University, Melbourne, Victoria 3001, Australia

Graphical abstract

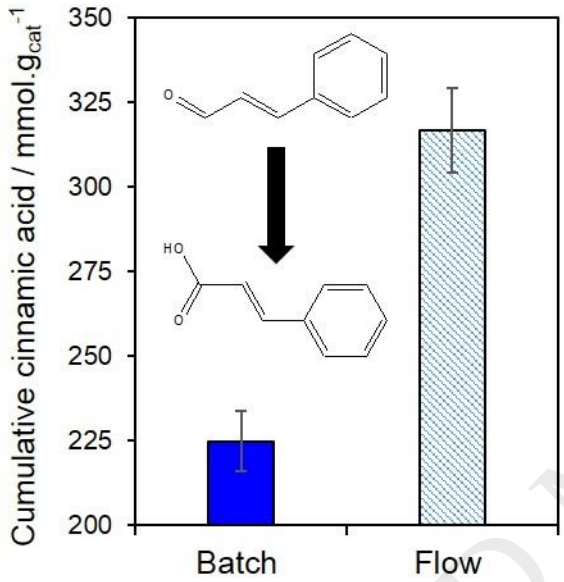

Highlights

- Silica supported Pt nanoparticles are active and selective for base-free cinnamaldehyde aerobic oxidation
- High area, mesoporous silica supports increase Pt dispersion and hence activity and cinnamic acid yield
- Surface PtO_2 is the active site for selective oxidation of cinnamaldehyde→cinnamic acid
- Continuous flow operation stabilises surface PtO_2 thereby significantly enhancing catalyst stability and acid yield

Abstract

Aerobic selective oxidation of allylic aldehydes offers an atom and energy efficient route to unsaturated carboxylic acids, however suitable heterogeneous catalysts offering high selectivity and productivity have to date proved elusive. Herein, we demonstrate the direct aerobic oxidation of cinnamaldehyde to cinnamic acid employing silica supported Pt nanoparticles under base-free, batch and continuous flow operation. Surface and bulk characterisation of four families of related Pt/silica catalysts by XRD, XPS, HRTEM, CO chemisorption and N_2 porosimetry evidence surface PtO_2 as the common active site for cinnamaldehyde oxidation, with a common turnover frequency of 49,000±600 h^{-1}; competing cinnamaldehyde hydrogenolysis is favoured over metallic Pt. High area mesoporous (SBA-15 or KIT-6) and macroporous-mesoporous SBA-15 silicas confer significant rate and cinnamic acid yield enhancements versus low area

fumed silica, due to superior platinum dispersion. High oxygen partial pressures and continuous flow operation stabilise PtO_2 active sites against in-situ reduction and concomitant deactivation, further enhancing cinnamic acid productivity.

Keywords: Platinum; Cinnamaldehyde; Oxidation; Porous; Silica

1. Introduction

The aerobic selective oxidation (selox) of aldehydes represents an environmentally benign and atom efficient molecular transformation for chemical valorisation [1], affording the production of complex α, β-unsaturated acids (and their esters) under mild conditions [2]. Such acids are valuable chemical products and intermediates, for example cinnamic acid is important in the fine chemical and pharmaceutical sectors as a food [3] and perfume additive [4], as a precursor to the sweetener aspartame [5], and also finds application as an anti-fungal [6] and potential anti-malarial agent [7]. Traditionally, stoichiometric amounts of hazardous inorganic oxidants were utilised in selective alcohol and aldehyde oxidation, but this approach is considered unsustainable and hence alternative catalytic clean technologies are sought [8-10]. The presence of proximate C=C and C=O functionalities pose an especial challenge to achieving high selectivity to the unsaturated acid in such aerobic oxidations [11].

Platinum group metals (PGMs) are effective heterogeneous catalysts for aerobic selox of alcohol, aldehydes and carbohydrates, and the subject of numerous reviews [9, 12-15]. In this regard, α, β-unsaturated acids are typically prepared by the cascade oxidation of their corresponding alcohols under strongly basic conditions [16-19]. Platinum nanoparticles dispersed over oxide and carbon supports are widely studied for the aerobic selox of aliphatic [20-22], allylic [23-25] and benzylic [26, 27] primary and secondary alcohols and carbohydrates [28, 29], but typically utilise p-block promoters such as Bi, Pd, Sn and Te [19, 23] under basic conditions. Nevertheless, the nature of the active site and role(s) of promoters and base remain poorly understood, reflecting the complex solid-liquid-gas interface and necessity for (but attendant difficulties in performing and interpreting) in-situ/operando studies on supported metal catalysts for aerobic selox [30, 31]. Recent spectroscopic and kinetic studies of cinnamyl alcohol aerobic oxidation over silica supported Pt nanoparticles identified surface PtO_2 as the active site for the selective production of cinnamaldehyde [32]. Hydrogen adatoms liberated during this oxidative dehydrogenation drive in-situ reduction of surface platinum oxide, with the resulting Pt^0 sites favouring styrene formation through hydrogenolysis of the C-C bond, and production of the saturated 3-phenylpropanoic acid [33]. It is interesting to note that cationic Pt is also proposed as the active species in the aerobic oxidative dehydrogenation of shikimic acid to dehydroshikimic acid over a platinum tetrasulfophthalocyanine catalyst [34]. These observations mirror palladium analogues, wherein surface PdO adlayers [35-37] and electron deficient Pd single atoms [38] are now recognised as the catalytically active species in allylic alcohol selox.

In contrast to alcohol selox, there are scant reports of the direct aerobic oxidation of unsaturated aldehydes over PGMs, these being restricted to the cascade oxidation of 5-hydroxymethylfurfural, for which Pt catalysts again require additional inorganic base (liquid or solid [39]) and/or promoters [40, 41] to achieve significant yields of 2,5-furandicarboxylic acid (2,5-FDCA). There are also few examples of heterogeneously catalysed, liquid phase aerobic oxidations in continuous flow [42-45], despite the attendant process advantages for atom economical, and scalable, organic synthesis. In the context of platinum, aerobic flow oxidation of primary and secondary alcohols to their corresponding carboxylic acids is reported over Pt nanoparticles dispersed in an amphiphilic polymer resin at high oxygen pressures (40-70 bar) and temperature (100-120 °C), which are undesirable from the perspective of developing a

sustainable process, and for Pt/Al_2O_3 in a trickle-bed reactor for ethanol and benzyl alcohol oxidation [46] albeit minimal information was provided on product selectivity.

Herein, we report one of the first examples of Pt catalysed aerobic selox of α, β-unsaturated aldehydes, under mild and base-free conditions, and highlight the influence of support architecture, Pt oxidation state, and reaction conditions on the yield of cinnamic acid from cinnamaldehyde. Significant productivity enhancements are also demonstrated for continuous flow versus batch cinnamaldehyde oxidation to cinnamic acid.

2. Experimental

2.1 Catalyst synthesis

2.1.1 SBA-15 synthesis. 10 g Pluronic P123 was dissolved in 75.5 cm^3 water and 291.5 cm^3 of 2 M hydrochloric acid under stirring at 35 °C. 15.5 cm^3 Tetraethylorthosilicate was subsequently added and left stirring for 20 h. The resulting gel was aged for 24 h at 80 °C without agitation. The solid was filtered, washed with 1000 cm^3 water, and dried at room temp before calcination at 500 °C for 6 h in air (ramp 1 $°C.min^{-1}$). The resulting silica exhibited the expected ordered, hexagonal (*p6mm*) arrangements of monodispersed, uniform mesopores.

2.1.2 KIT-6 synthesis. 10g Pluronic F127 was dissolved in 361.6 cm^3 water, 12.3 cm^3 butan-1-ol and hydrochloric acid (35%, 16.7 cm^3) with stirring at 35 °C. 15.6 cm^3 Tetramethoxysilane was added and left for 20 h with agitation. The resulting gel was aged for 24 h at 80 °C without agitation. The solid was filtered, washed with 1000 cm^3 water and dried at room temperature before calcination at 500 °C for 6 h in air (ramp rate 1 $°C.min^{-1}$). The resulting silica exhibited the expected gyroidal pore architecture (Ia3d symmetry) with interconnecting pore channels.

2.1.3 Polystyrene colloidal nanospheres. Polystyrene nanospheres were synthesised by the method of Vaudreuil and co-worker, employing styrene (Sigma Aldrich, >99 %) as the monomer source and potassium persulphate (Sigma Aldrich, >99 %) as the initiator, in a 2 L Radleys Reactor Ready jacketed glass reactor at 80 °C. 103 cm^3 of styrene was washed five times with 0.1 M NaOH and deionised water to remove polymerisation inhibitors, and added to 1.275 L of deionised water previously degassed overnight in the reactor under 1.5 bar flowing N_2 (10 $cm^3.min^{-1}$). Subsequently, 0.33 g of potassium persulphate was dissolved in 50 cm^3 deionised water at 70 °C and added to the styrene mixture to initiate polymerisation, and stirred at 300 rpm under flowing N_2 for 22 h. The resultant solid was recovered, filtered and washed three times with deionised water, and a further three times with ethanol. The polystyrene nanospheres obtained were dried overnight at 80 °C to yield a final dry mass of approximately 70 g.

2.1.4 Macro-mesoporous SBA-15 synthesis. Hierarchical macroporous-mesoporous SBA-15 was synthesised by a dual hard-soft templating approach. An organic mesophase was first prepared through True Liquid Crystal Templating by mixing 2 g Pluronic P123 with 2 g of 2M HCl acidified water (pH 2) and subsequent ultrasonication for 3 h at 40 °C to produce a homogeneous gel. To this, 4.08 cm^3 of aqueous tetramethoxysilane (1:4 molar ratio in H_2O) was added and mixed, yielding a homogeneous liquid. 6 g of polystyrene colloidal nanospheres was subsequently added to this solution, and the resulting mixture heated at 40 °C in vacuo (100 mbar) overnight to obtain a viscous gel. The gel was aged for 24 h at room temperature to fully condense the silica framework, and then calcined at 500 °C (ramp rate $1°C.min^{-1}$) for 6 h in static air.

2.1.5 Platinum impregnation. Wet impregnation of 2 g each of mesoporous SBA-15, KIT-6 and MM-SBA-15 silicas, and a commercial fumed silica (Sigma Aldrich S5505, 200 $m^2.g^{-1}$), was performed with 16 cm^3 aqueous ammonium tetrachloroplatinate (II) solution (precursor concentrations adjusted to achieve nominal Pt loadings of 0.05-2 wt%). The resulting slurries were stirred for 18 h at room temperature before heating to 50 °C. After a further 5 h agitation, the

remaining solids were held at 50 °C for 24 h to obtain dry powders, which were then calcined at 500 °C (ramp rate 1 °C.min^{-1}) for 2 h in static air, prior to reduction at 400 °C (ramp rate 10 °C.min^{-1}) for 2 h under 10 cm^3.min^{-1} flowing hydrogen. Reference 0.5 wt% Pt catalysts were also prepared by wet impregnation as described above on P25 (Sigma-Aldrich, 99.5 %) and Degussa C γ-alumina (>99.8 %) supports, to examine the impact of support reducibility.

2.2 Characterisation

Nitrogen porosimetry was undertaken on a Quantachrome Nova 2000e porosimeter using NovaWin version 11 analysis software. Samples were degassed at 120 °C for 2 h prior to nitrogen physisorption. Adsorption/desorption isotherms were recorded for parent and Pt impregnated silicas, with BET surface areas calculated over the relative pressure range 0.01-0.2. Pore diameters and volumes were calculated by applying the BJH method to desorption isotherms for relative pressures >0.35. Wide angle XRD patterns were recorded on a Bruker D8 Advance diffractometer with a Cu K_α (1.54 Å) source calibrated against a Si standard, between 2θ = 20-90 ° with a step size of 0.02 °. The Scherrer equation was used to calculate volume-averaged Pt particle sizes from line broadening. Low angle XRD patterns were recorded for 2θ = 0.5-2.5 ° with a step size of 0.02 °. XPS was performed on a Kratos Axis HSi X-ray photoelectron spectrometer fitted with a charge neutraliser and magnetic focusing lens employing Al K_α monochromated radiation (1486.7 eV). Spectral fitting was performed using CasaXPS version 2.3.14, with binding energies corrected to the C 1s peak at 284.6 eV. Pt 4f XP spectra were fitted using an asymmetric lineshape. Pt nanoparticle dispersion as measured via CO pulse chemisorption on a Quantachrome ChemBET3000 system. Catalysts were outgassed at 150 °C under 20 cm^3.min^{-1} flowing He for 1 h, prior to 150 °C reduction under 10 cm^3.min^{-1} flowing hydrogen for 1 h and subsequent room temperature analysis. CO:$Pt_{surface}$ stoichiometry of 0.68 was assumed, since the formation of a fully saturated monolayer is energetically unfavourable under these measurement conditions. This reduction protocol is milder than that employed during wet impregnation, and does not induce additional particle sintering. Metal loading was determined by EDX analysis on a Carl Zeiss Evo-40 SEM operated at 25 Kv. High resolution high-angle annular dark-field STEM images were obtained on an aberration-corrected JEOL 2100-F microscope operated at 200 kV, with image analysis using ImageJ 1.41 software. Samples were dispersed in methanol and drop cast on 200-mesh carbon coated copper grids and dried under ambient conditions.

2.3 Catalyst testing

2.3.1 Batch oxidation. Catalysts were tested in a Radleys StarFish carousel reactor on a 10 cm^3 scale. 50 mg catalyst was added to a reaction mixture containing 8.4 mmol cinnamaldehyde (1.11 g), 0.1 cm^3 mesitylene as an internal standard, and 10 cm^3 toluene solvent preheated to 90 °C under 1 bar of bubbling O_2 (5 cm^3.min^{-1}). The Pt concentration varied between 0.13 and 5.4 μmol (for 0.05-2.10 wt% Pt loadings), corresponding to substrate:catalyst ratios ranging from 6.55 x 10^4 to 1.56 x 10^3. Reactions were sampled periodically for by off-line gas chromatography using a Varian 3900GC with 8400 autosampler fitted with a CP-Sil5 CB column (15 m x 0.25 mm x 0.25 μm). High pressure (1-10 bar O_2) oxidations were performed in a Parr 5513 100 cm^3 stainless steel stirred autoclave fitted with a dip-tube for the 0.52 wt% Pt/SBA-15 catalyst using a substrate:catalyst ratio of 1.25 x 10^4 to ensure accurate kinetic analysis. In both reactors, control experiments showed negligible substrate conversion (for all screened substrates) in the absence of either O_2 or platinum catalyst. Oxidation rates (and selectivity) were zero order with respect to catalyst mass, confirming reactions were free from bulk or in-pore mass-transport limitations. Hot filtration experiments evidenced negligible Pt leaching, confirming the heterogeneous nature of the observed reactivity. Activity and selectivity values are the mean of duplicate or triplicate reactions, with errors of ±3 % and mass balances >96 % in all cases. Conversion was calculated from **Equation 1**, where

n_t is the number of mmol cinnamaldehyde at time t, and n_0 the initial mmol cinnamaldehyde, and selectivity calculated from **Equation 2** based exclusively on the five major liquid phase products, where $n_{x=i}$ is the mmol of product *i* (cinnamic acid, 3-phenylpropan-1-ol, styrene, cinnamyl esters or cinnamyl alcohol) and Σn_x denotes the total mmol of all products. Yield was calculated from **Equation 3**. Mass-normalised initial rates were calculated from the first hour of reaction, and Turnover Frequencies (TOFs) calculated from **Equation 4** by normalising raw initial rates to the mmol surface Pt species determined from CO dispersion and XPS.

$$\% \text{ Conversion} = [(n_0 - n_t) / (n_0)] \times 100 \qquad \textbf{Equation 1}$$

$$\% \text{ Selectivity} = [(n_{x=i}) / (\Sigma n_x)] \times 100 \qquad \textbf{Equation 2}$$

$$\% \text{ Yield} = [\text{Conversion} \times \text{Selectivity}) / 100 \qquad \textbf{Equation 3}$$

$$\text{TOF} = \text{mmol}_{\text{Cinnamaldehyde}} \text{ converted.h}^{-1} / \text{mmols surface Pt}^{0 \text{ or } x+} \qquad \textbf{Equation 4}$$

2.3.2 Flow oxidation. Catalyst testing was conducted using a Uniqsis FlowSyn reactor, comprising a GAM II gas-liquid addition module and packed-bed microreactor with downstream backflow pressure regulator [47]. An integral HPLC pump delivered a liquid stream of 0.84 M cinnamaldehyde in toluene (with mesitylene as internal standard) at flow rates between 0.1-2.0 $cm^3.min^{-1}$, while 40 cm^3 oxygen gas flow was delivered via an in-line Brooks mass flow controller and back pressure regulator. Liquid and gas feeds were pre-mixed before introduction to the catalyst bed via the GAM II module, which features a semi-permeable polymer coil and reactor mandrel heated to 90 ˚C to ensure efficient gas-liquid mixing and heating to prior to contact with the catalyst. 50 mg of catalyst was diluted with quartz beads (Sigma Aldrich, mesh size = -325) to minimise back pressure, and packed within a 10 mm i.d. x 100 mm OMNIFIT® glass column to give a total bed volume of 2.5 cm^3, held within the glass reactor by quartz wool plugs. The reactor was vertically mounted and the gas-saturated liquid stream fed in an up-flow direction to minimise catalyst settling and maximise permeation through the catalyst bed. Neither fluidisation nor compaction of the catalyst bed was observed. The exit stream passed through a needle valve and backflow regulator, with excess gas vented prior to sampling for off-line GC analysis.

3. Results and discussion

3.1 Catalyst characterisation

Four families of Pt catalysts were synthesised employing amorphous, ordered mesoporous (SBA-15 and KIT-6), or hierarchical microporous-mesoporous (MM-SBA-15) silicas to elucidate the impact of support architecture on their physicochemical properties, and the subsequent selective aerobic oxidation of cinnamaldehyde. Mesoporous SBA-15 (*p6mm*) and KIT-6 (*Ia3d*) architectures were identified through indexing their characteristic low angle powder X-ray diffraction (XRD) patterns (**Figure S1**), however macropore incorporation disrupts extended SBA-15 ordering, preventing the collection of a corresponding (high quality) low angle XRD pattern for the MM-SBA-15 support. Calculated cell parameters and wall thicknesses for the mesoporous and hierarchical supports (**Table S1**) are in accordance with the literature [48-50]. Nitrogen porosimetry confirmed the expected type IV isotherms and type I hysteresis for the mesoporous and hierarchical supports (**Figure S2**), and corresponding high BET surface area and narrow BJH mesopore size distributions (**Table S1** and **Figure S2**). In contrast, the commercial silica exhibited a type II isotherm, reflecting a disordered pore network, and low BET surface area. High resolution transmission electron microscopy (HRTEM) in **Figure 1** shows hexagonal close-packed mesopores for SBA-15 [49], cubic close-packed

mesopores for KIT-6 [48], and the incorporation of 300 nm macropores between hexagonal close-packed mesopore channels in MM-SBA-15 [50].

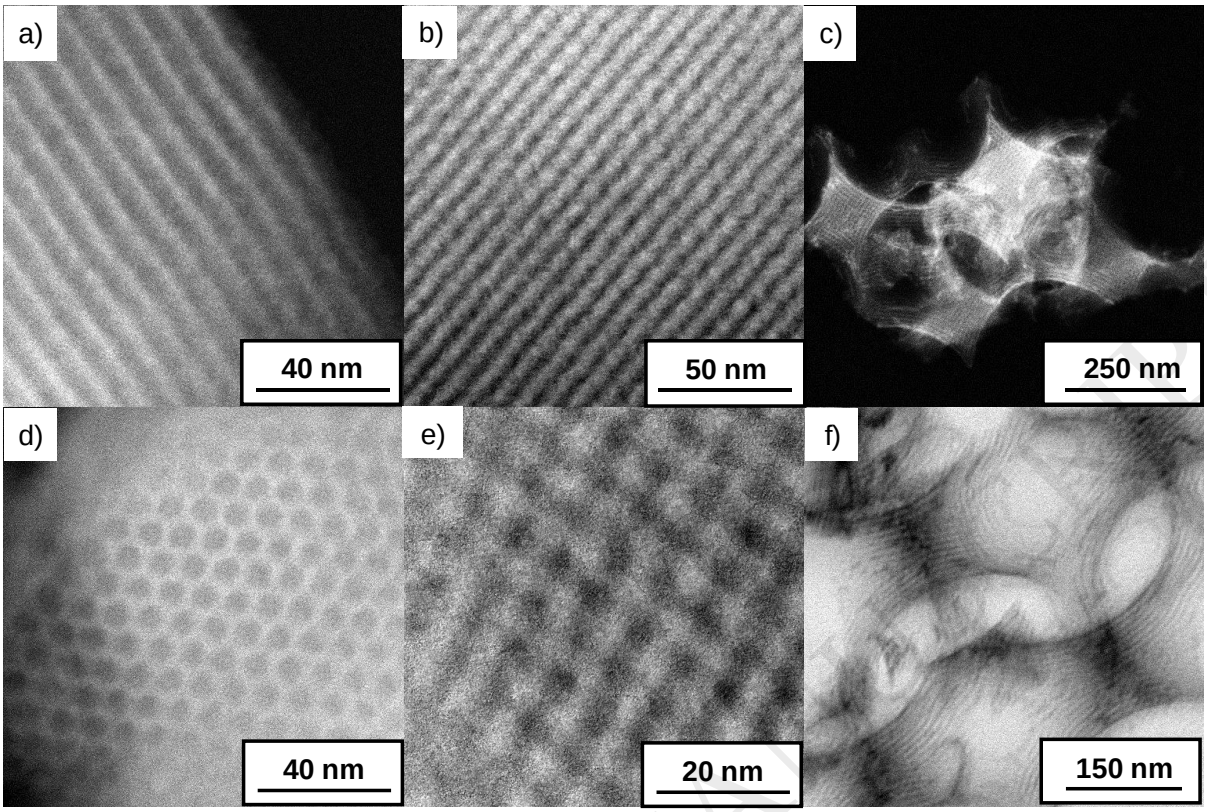

Figure 1. HRTEM dark (top) and bright (bottom) field images of (a,d) SBA-15, (b,e) KIT-6, and (c,f) MM-SBA-15 silicas.

Physicochemical characteristics of the Pt/silica analogues are summarised in **Table S2**, and are in excellent agreement with literature reports [32, 51, 52]. XRD, HRTEM and N_2 porosimetry confirmed retention of the parent silica pore structures following platinum impregnation (**Table S2, Figure S3-4)**, but a loss of BET surface area and pore volume proportional to Pt loading, attributed to partial pore blockage, as previously observed. The smaller magnitude of surface area decrease observed for the fumed SiO_2 catalysts upon Pt impregnation is consistent with nanoparticle deposition primarily on the external surface. Metal dispersion (determined by CO chemisorption) was inversely proportional to Pt loading for all supports (**Table S2**), with particle sizes (determined by a combination of TEM, wide angle XRD (**Figure S5**) and CO chemisorption) proportional to the silica surface area and spanning 1.7 nm (0.07 wt% Pt/KIT-6) to 15.6 nm (2.10 wt%/fumed SiO_2). The degree of platinum surface oxidation, as measured by XPS, was directly proportional to Pt dispersion, as previously reported [32, 52] (**Figure S7-8)**, associated with the formation of PtO_2, with a Pt $4f_{7/2}$ binding energies of 74.5 eV [32, 52-54] over smaller nanoparticles. Platinum surface oxidation was support dependent decreasing in the order: KIT-6 > SBA-15 > MM-SBA-15 > fumed SiO_2 (**Table S2**).

3.2 Batch oxidation of cinnamaldehyde

Cinnamaldehyde aerobic selox was subsequently investigated over the preceding four families of Pt/silica catalysts. Control experiments showed negligible aldehyde conversion in the absence of supported platinum and/or O_2, while hot filtration tests and elemental analysis of filtrate and spent catalysts revealed negligible platinum leaching (**Figure S9**).

All reactions were performed at 800 rpm, and were zero order with respect to mass-normalised catalyst activity (and selectivity), evidencing that oxidations were free from external mass-transport limitations (**Figure S10** and **S11**). Reaction profiles are shown in **Figure S12**. Initial rates of cinnamaldehyde selox were inversely proportional to Pt loading for all supports (**Figure 2a**), with activity proportional to platinum dispersion and hence surface PtO_2 concentration (**Figure S13**): KIT-6 > SBA-15 > MM-SBA-15 > fumed SiO_2, consistent with observations for both Pd and Pt catalysed aerobic selox of cinnamyl alcohol to cinnamaldehyde [32, 55, 56]. Turnover frequencies (TOFs) for cinnamaldehyde selox normalised per surface PtO_2 site were 49,000 h^{-1}, independent of Pt loading or silica support (**Figure 2b**): this demonstrates that (i) PtO_2 is the active site for cinnamaldehyde aerobic selox (and not Pt metal); and (ii) the superior activity of the mesoporous and hierarchical catalysts does not arise from enhanced in-pore mass transport, but is solely associated with higher Pt dispersion.

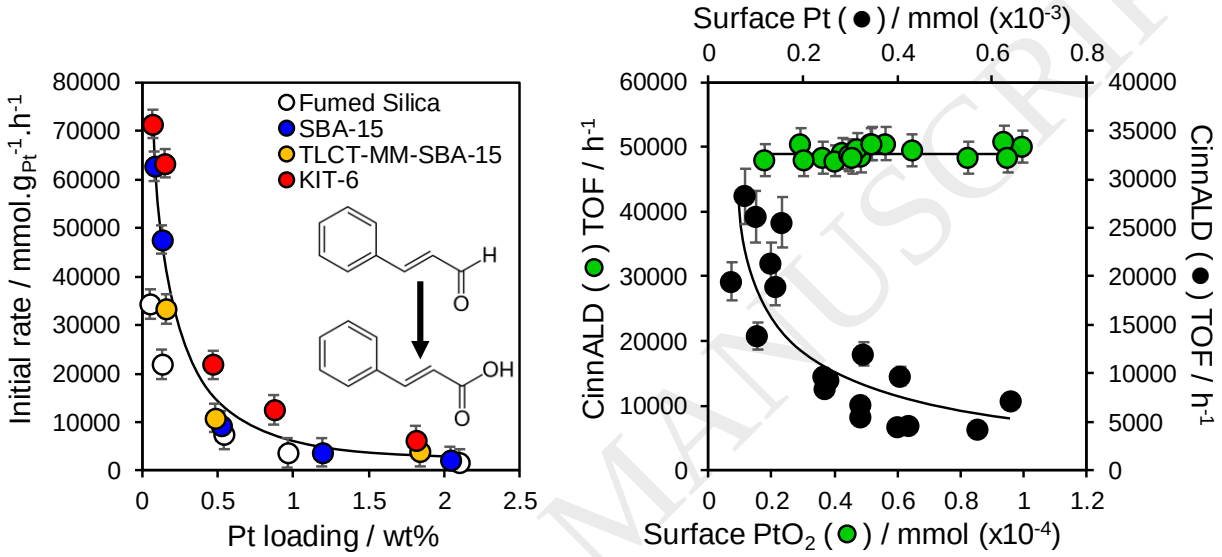

Figure 2. (*left*) Mass-normalised initial rates and (*right*) corresponding turnover frequencies for cinnamaldehyde aerobic selox over 0.05-2.1 wt% Pt/silica catalysts. Reaction conditions: 50 mg catalyst, 8.4 mmol cinnamaldehyde in 10 cm^3 toluene, 5 $cm^3.min^{-1}$ bubbling O_2 at 1 bar, 90 °C, and 800 rpm stirring.

Figure 3 shows the striking performance enhancements attainable through tailoring the support porosity and surface area, which deliver a three-fold increase in mass-normalised activity and an absolute increase of 11 % in cinnamic acid yield for 0.15 wt% Pt/silicas by substituting a fumed SiO_2 for a KIT-6 support. These Pt/silicas are effective catalysts for the production of α, β-unsaturated acids, aliphatic and aromatic acids by aerobic oxidation (**Table S3**).

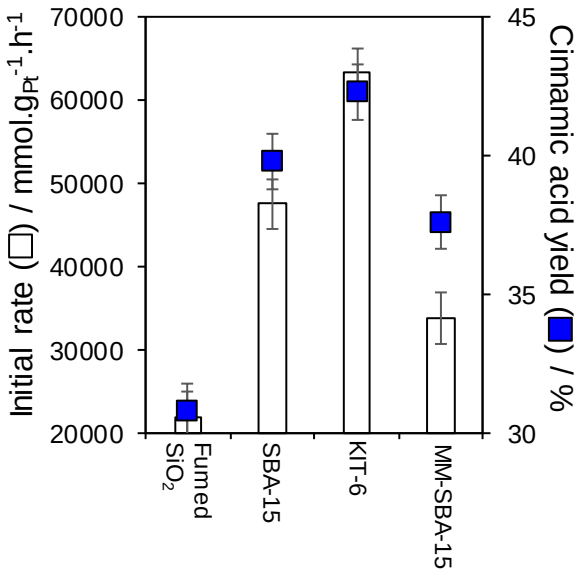

Figure 3. Comparison of initial rates and 5 h cinnamic acid yields for cinnamaldehyde aerobic selox over 0.15 wt% Pt/silica catalysts as a function of support architecture. Reaction conditions: 50 mg catalyst, 8.4 mmol cinnamaldehyde in 10 cm^3 toluene, 5 $cm^3.min^{-1}$ bubbling O_2 at 1 bar, 90 °C, and 800 rpm stirring.

Figure 4 shows the product distribution as a function of surface PtO_2 concentration, and confirms oxidised platinum as the active catalytic species for cinnamaldehyde aerobic selox to cinnamic acid, whereas metallic platinum favours cinnamaldehyde decarbonylation to styrene (or hydrogenation to 3-phenylpropan-1-ol); note we have been previously shown cinnamic acid does not undergo decarboxylation to styrene over Pt/silica catalysts under identical conditions [32]. Decarbonylation of reactively-formed aldehydes during aerobic selox of alcohols over Pt catalysts, and resulting site blocking by strongly-bound CO, is reported as a major cause of catalyst deactivation in such systems [57-60]. Complementary studies by Zaera and co-workers over Pt(111) single crystal model catalysts reveal that crotonaldehyde (a simple allylic aldehyde) binds to the metal surface through the C=C moiety, inducing extensive rehybridization of the double bond, weakening conjugation and promoting decarbonylation to adsorbed CO and gaseous propene on thermal treatment [61]. **Figures 2-4** suggest that the deactivation and poor selectivity to aldehydes/acids that plagues platinum selox catalysts reflects their low nanoparticle dispersion and hence metallic surfaces. The importance of maintaining platinum in an oxidised state was further evidenced by the impact of a mild pre-reduction treatment on the performance of the 0.52 wt% Pt/SBA-15 catalyst (**Figure S14**). Pre-reduction suppressed the initial activity and 5 h conversion by 43 % and 25 % respectively for cinnamaldehyde aerobic selox, and lowered the cinnamic acid yield by 37 % at the expense of increased styrene production. Furthermore, **Figure S15** evidences a linear relationship between the surface PtO_2 concentration and ratio of cinnamic acid:by-products. Our hypothesis that surface PtO_2 is the active and selective site for cinnamaldehyde oxidation to cinnamic acid is also supported by the significant increase in aldehyde conversion (from 36→86 %) and acid selectivity (67→86 %) observed on raising the pO_2 from 1 →10 bar over 0.52 wt% Pt/SBA-15. XPS and CHN analysis of fresh and spent 0.52 wt% Pt/silica following 5 h cinnamaldehyde aerobic selox confirm that higher pO_2 stabilise PtO_2 and restrict site-blocking by strongly-bound organic products/residues (**Figure S16**). Analogous improvements in conversion and selectivity with increasing oxygen pressure are reported in the aerobic selox of glucose to glucaric acid over Pt/C [62]. Note that it is difficult to develop a quantitative relationship between the oxygen partial pressure and surface PtO_2 concentration, since catalytically active surface oxides formed by platinum under high O_2

pressures (1-5 bar) are only metastable [63]. This likely explains the non-linear relationship in **Figure S16** between the increase in surface PtO_2 oxide determined ex-situ by XPS post-reaction from 7.0→11.4 wt% upon raising the pO_2 employed during oxidation from 1→10 bar. Accurate quantification of the PtO_2 content at elevated pressures would require a liquid phase operando XAS study, which will be the subject of future investigations.

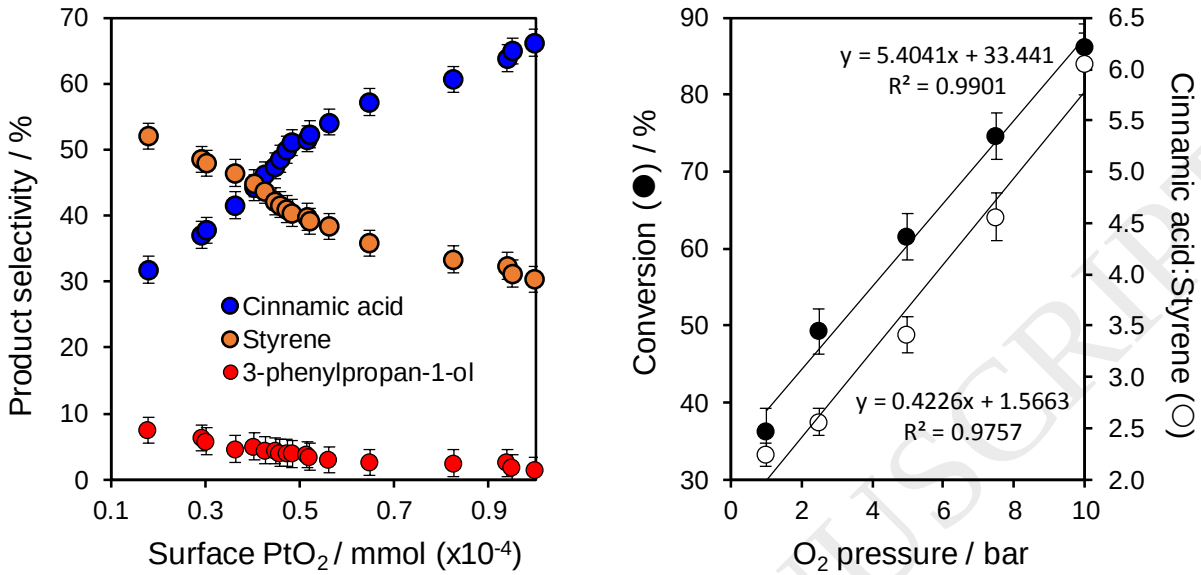

Figure 4. (*left*) Influence of surface PtO_2 concentration on 5 h product selectivity for cinnamaldehyde aerobic selox over Pt/silicas at 1 bar O_2, and (*right*) influence of pO_2 on 5 h cinnamaldehyde conversion and cinnamic acid:styrene selectivity over 0.52 wt% Pt/SBA-15 catalyst. Reaction conditions: 50 mg catalyst, 16.8 mmol cinnamaldehyde in 10 cm^3 toluene, 90 °C, and 800 rpm stirring.

Having identified PtO_2 as the active site in cinnamaldehyde aerobic selox, the question naturally arises as to whether higher active site densities, and hence activity, might be favoured by more reducible oxide supports which interact more strongly with platinum (and hence should enhance its dispersion and PtO_2 stability). **Figure 5** confirms this hypothesis, with the mass-normalised initial rates of 0.5 wt% Pt wet-impregnated over different oxide supports decreasing in the order TiO_2 > Al_2O_3 > fumed SiO_2, closely mirroring the proportion of surface PtO_2 in each catalyst.

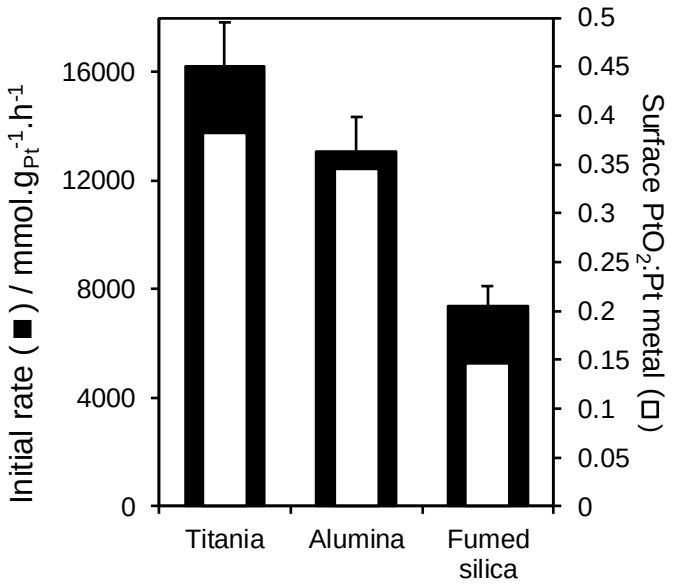

Figure 5. Comparison of mass-normalised initial rates of cinnamaldehyde aerobic selox over 0.52 wt% Pt catalysts as a function of support, and corresponding degree of surface platinum oxidation determined by XPS of fresh catalysts. Reaction conditions: 50 mg catalyst, 8.4 mmol cinnamaldehyde in 10 ml toluene, 5 $cm^3.min^{-1}$ bubbling O_2 at 1 bar, 90 °C, and 800 rpm stirring.

Cinnamaldehyde aerobic selox over shows a moderate temperature dependence (reflected by an apparent activation energy of 29±2 $kJ.mol^{-1}$, **Figure S17**), with conversion increasing from 20→70 % over the 0.52 wt% Pt/SBA-15 catalyst with increasing reaction temperature from 20-90 °C, however additional heating lowered activity possibly associated with lower oxygen solubility (**Figure 6**). Cinnamic acid and styrene production mirrored reactant conversion albeit with a slightly weaker temperature dependence, and indeed exhibit similar apparent activation energies of 24±2 and 27±2 $kJ.mol^{-1}$ respectively. The latter is in reasonable agreement with DFT calculations for furfural decarbonylation over a Pt_{55} cluster of 35 $kJ.mol^{-1}$ [64]. In contrast, 3-phenylpropan-1-ol production was weakly temperature dependent, increasing slightly above 90 °C. High reaction temperatures therefore favoured decarbonylation (and C=C/C=O hydrogenation), as previously observed during alcohol aerobic selox [57, 65], and which we attribute to PtO_2 reduction to metallic Pt at elevated temperature (**Figure S16**) [66].

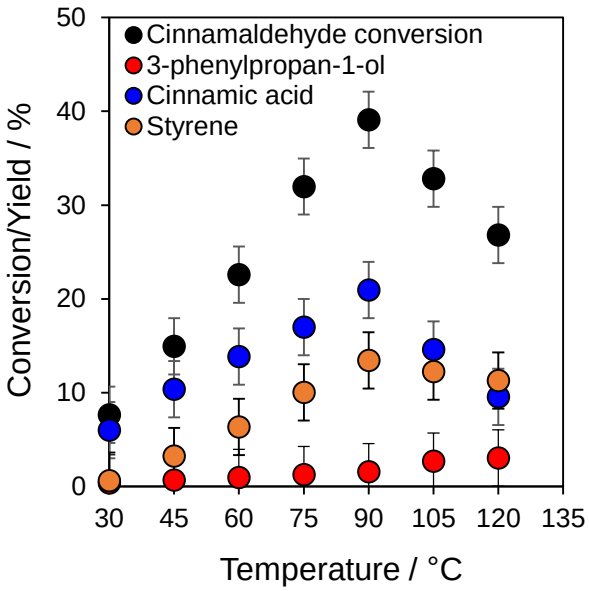

Figure 6. Influence of reaction temperature on conversion and 1 h product yield for cinnamaldehyde aerobic selox over 0.52 wt% Pt/SBA-15 catalyst. Reaction conditions: 50 mg catalyst, 8.4 mmol cinnamaldehyde in 10 cm^3 toluene, 5 $cm^3.min^{-1}$ bubbling O_2 at 1 bar, 90 °C, and 800 rpm stirring.

3.3. Continuous flow oxidation of cinnamaldehyde

The potential for scale-up and impact of continuous versus batch process operation was subsequently assessed for cinnamaldehyde aerobic selox over the 0.52 wt% Pt/SBA-15 catalyst under the optimum reaction conditions determined in Section 3.2 (90 °C and 10 bar O_2). Cinnamaldehyde conversion (**Figure S18**) and product selectivity (**Figure 7a**) were first determined as a function of residence time (τ). Negligible cinnamaldehyde conversion was observed for $\tau < 5$ min, with longer residence times resulting in a monotonic increase in activity, with single pass conversions reaching a plateau of 60 % for $\tau > 25$ min, likely due to limited oxygen availability under these conditions. Cinnamic acid production displayed a volcano dependence on residence time, reaching a maximum of 84 % for $\tau = 17$ min. In contrast, 3-phenylpropan-1-ol production exhibited a monotonic decrease with residence time, concomitant with a monotonic increase with styrene production, suggesting these undesired by-products are formed by competing pathways that share a common active site (which the preceding batch oxidations indicate is metallic surface Pt). The fall in cinnamic acid selectivity at the expense of styrene observed at long residence times is attributed oxygen starvation and consequent in-situ reduction of surface PtO_2, which **Figure 4a** shows is the active site for cinnamaldehyde oxidation. Catalyst stability was subsequently evaluated for $\tau = 17$ min, the optimum residence time for cinnamic acid production, as a function of time-on-stream (**Figure S19** and **S20**). Negligible deactivation was observed over 7 h continuous flow operation, in contrast with a batch reaction under comparable conditions in which 60 % of the initial activity was lost over the same period, consistent with **Figure S16** which shows greater carbon deposition and in-situ reduction of PtO_2 in batch; XRD confirmed deactivation in batch was not due to particle sintering (**Figure S21**). High selectivity to cinnamic acid (84 %) was also maintained in continuous flow, whereas deactivation on-stream in batch was accompanied by a slow, but continuous switchover from cinnamic acid to styrene production. Cumulative 7 h cinnamic acid production in batch and continuous flow is compared in **Figure 7b**, revealing a 37 % increase in cinnamaldehyde→cinnamic acid is attainable by flow operation.

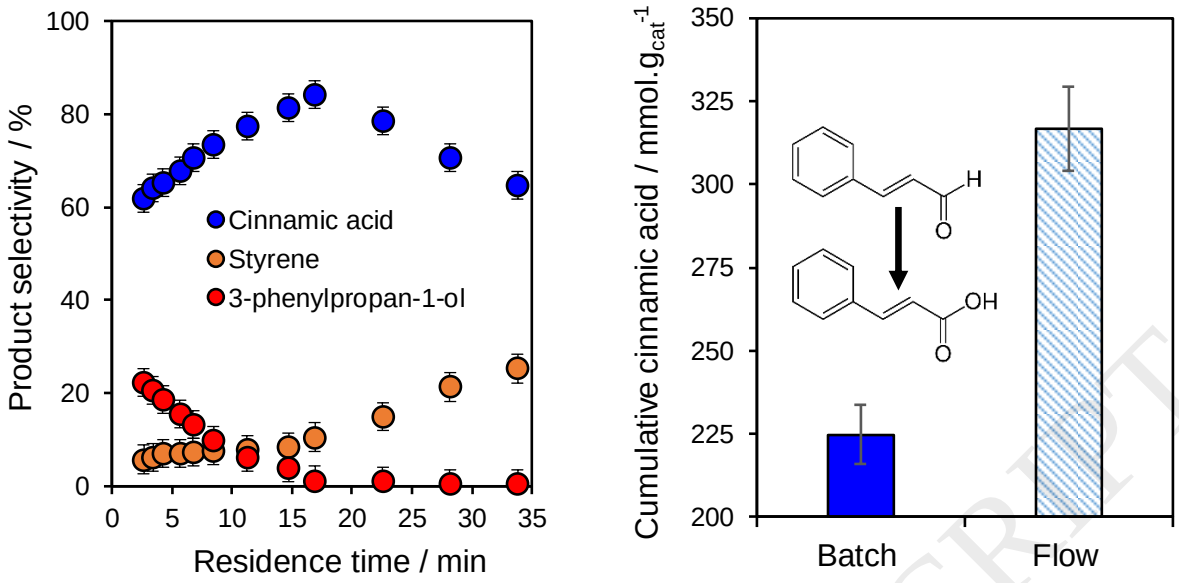

Figure 7. (*left*) Influence of residence time on selectivity for cinnamaldehyde aerobic selox over 0.52 wt% Pt/SBA-15 in continuous flow, and (*right*) cumulative 7 h cinnamic acid yield for cinnamaldehyde aerobic selox over 0.52 wt% Pt/SBA-15 in batch versus continuous flow. Reaction conditions: 50 mg catalyst, 16.8 mmol cinnamaldehyde in 10 cm^3 toluene (batch)/0.84 M (flow), 10 bar O_2 (static batch, 40 cm^3/min^{-1} flow), 90 °C, 800 rpm stirring (batch)/0.2 $cm^3.min^{-1}$ liquid feed (flow).

4. Conclusions

The influence of support architecture and process conditions on the heterogeneously catalysed liquid phase selective aerobic oxidation of cinnamaldehyde to cinnamic acid was investigated over silica supported Pt nanoparticles. In all cases, activity was directly proportional to nanoparticle dispersion and the degree of platinum oxidation. Surface PtO_2 is identified as the active site responsible for cinnamic acid production, with in-situ reduction promoting cinnamaldehyde decarbonylation to styrene (and a minor hydrogenation pathway to 3-phenylpropan-1-ol) over metallic Pt; increasing the oxygen partial pressure from 1→10 bar suppresses the later undesirable side-reactions and enhances cinnamic acid productivity (80 % selectivity and 74 % yield after 5 h at 90 °C). Mesoporous, high area silica supports significantly increase the concentration of active and selective surface PtO_2 catalytic species, and hence cinnamic acid yield, relative to commercial fumed silica, offering a simple approach to precious metal thrifting [67]. Pt/SBA-15 is also active and selective for production of aliphatic and aromatic acids from their corresponding aldehydes. Continuous flow operation improves catalyst stability, completely suppressing on-stream deactivation observed in batch, and thereby maintaining a high PtO_2 concentration (and hence selectivity to the α, β-unsaturated acid of 84 %), resulting in a 37 % increase in net cinnamic acid productivity over 7 h reaction.

Declarations of interest: none

Acknowledgements

Funding: This work was supported by the EPSRC (EP/G007594/4, EP/K014749/1 and EP/K014676/1). We thank Professor Richard Palmer and Birmingham University for access to TEM facilities.

References

[1] J.R. McNesby, C.A. Heller, Oxidation of Liquid Aldehydes by Molecular Oxygen, Chemical Reviews, 54 (1954) 325-346.
[2] B.S. Bal, W.E. Childers, H.W. Pinnick, Oxidation of α, β-un saturated aldehydes, Tetrahedron, 37 (1981) 2091-2096.
[3] D.R.A. Muhammad, D. Praseptiangga, D. Van de Walle, K. Dewettinck, Interaction between natural antioxidants derived from cinnamon and cocoa in binary and complex mixtures, Food Chemistry, 231 (2017) 356-364.
[4] D. Belsito, D. Bickers, M. Bruze, P. Calow, H. Greim, J. Hanifin, A. Rogers, J. Saurat, I. Sipes, H. Tagami, A toxicologic and dermatologic assessment of related esters and alcohols of cinnamic acid and cinnamyl alcohol when used as fragrance ingredients, Food and Chemical Toxicology, 45 (2007) S1.
[5] C.T. Evans, C. Choma, W. Peterson, M. Misawa, Bioconversion of trans-cinnamic acid to L-phenylalanine in an immobilized whole cell reactor, Biotechnology and bioengineering, 30 (1987) 1067-1072.
[6] T.C. Lima, A.R. Ferreira, D.F. Silva, E.O. Lima, D.P. de Sousa, Antifungal activity of cinnamic acid and benzoic acid esters against Candida albicans strains, Natural Product Research, (2017) 1-4.
[7] V. Gayam, S. Ravi, Cinnamoylated chloroquine analogues: A new structural class of antimalarial agents, European Journal of Medicinal Chemistry, 135 (2017) 382-391.
[8] G.-J.t. Brink, I.W.C.E. Arends, R.A. Sheldon, Green, Catalytic Oxidation of Alcohols in Water, Science, 287 (2000) 1636-1639.
[9] T. Mallat, A. Baiker, Oxidation of Alcohols with Molecular Oxygen on Solid Catalysts, Chemical Reviews, 104 (2004) 3037-3058.
[10] C.P. Vinod, K. Wilson, A.F. Lee, Recent advances in the heterogeneously catalysed aerobic selective oxidation of alcohols, Journal of Chemical Technology & Biotechnology, 86 (2011) 161-171.
[11] Y. Wang, S. De, N. Yan, Rational control of nano-scale metal-catalysts for biomass conversion, Chemical Communications, 52 (2016) 6210-6224.
[12] M. Besson, P. Gallezot, Selective oxidation of alcohols and aldehydes on metal catalysts, Catalysis Today, 57 (2000) 127-141.
[13] J. Muzart, Palladium-catalysed oxidation of primary and secondary alcohols, Tetrahedron, 59 (2003) 5789-5816.
[14] R. Anderson, K. Griffin, P. Johnston, P.L. Alsters, Selective oxidation of alcohols to carbonyl compounds and carboxylic acids with platinum group metal catalysts, Advanced Synthesis & Catalysis, 345 (2003) 517-523.
[15] M.E. Ali, M.M. Rahman, S.M. Sarkar, S.B.A. Hamid, Heterogeneous Metal Catalysts for Oxidation Reactions, Journal of Nanomaterials, 2014 (2014) 23.
[16] M. Besson, G. Flèche, P. Fuertes, P. Gallezot, F. Lahmer, Oxidation of glucose and gluconate on Pt, Pt Bi, and Pt Au catalysts, Recueil des Travaux Chimiques des Pays-Bas, 115 (1996) 217-221.
[17] P. Korovchenko, C. Donze, P. Gallezot, M. Besson, Oxidation of primary alcohols with air on carbon-supported platinum catalysts for the synthesis of aldehydes or acids, Catalysis Today, 121 (2007) 13-21.
[18] B. Karimi, M. Khorasani, H. Vali, C. Vargas, R. Luque, Palladium nanoparticles supported in the nanospaces of imidazolium-based bifunctional PMOs: The role of plugs in selectivity changeover in aerobic oxidation of alcohols, ACS Catalysis, 5 (2015) 4189-4200.
[19] M.S. Ahmed, D.S. Mannel, T.W. Root, S.S. Stahl, Aerobic Oxidation of Diverse Primary Alcohols to Carboxylic Acids with a Heterogeneous Pd–Bi–Te/C (PBT/C) Catalyst, Organic Process Research & Development, 21 (2017) 1388-1393.
[20] R. Garcia, M. Besson, P. Gallezot, CHEMOSELECTIVE CATALYTIC-OXIDATION OF GLYCEROL WITH AIR ON PLATINUM METALS, Appl. Catal. A-Gen., 127 (1995) 165-176.
[21] S. Carrettin, P. McMorn, P. Johnston, K. Griffin, C.J. Kiely, G.J. Hutchings, Oxidation of glycerol using supported Pt, Pd and Au catalysts, Phys. Chem. Chem. Phys., 5 (2003) 1329-1336.
[22] Y. Kwon, T.J.P. Hersbach, M.T.M. Koper, Electro-Oxidation of Glycerol on Platinum Modified by Adatoms: Activity and Selectivity Effects, Top. Catal., 57 (2014) 1272-1276.

[23] T. Mallat, Z. Bodnar, P. Hug, A. Baiker, Selective Oxidation of Cinnamyl Alcohol to Cinnamaldehyde with Air over Bi-Pt/Alumina Catalysts, Journal of Catalysis, 153 (1995) 131-143.
[24] A.F. Lee, J.J. Gee, H.J. Theyers, Aspects of allylic alcohol oxidation - a bimetallic heterogeneous selective oxidation catalyst, Green Chem., 2 (2000) 279-282.
[25] Y. Kon, Y. Usui, K. Sato, Oxidation of allylic alcohols to alpha,beta-unsaturated carbonyl compounds with aqueous hydrogen peroxide under organic solvent-free conditions, Chemical Communications, (2007) 4399-4400.
[26] C. Mondelli, J.-D. Grunwaldt, D. Ferri, A. Baiker, Role of Bi promotion and solvent in platinum-catalyzed alcohol oxidation probed by in situ X-ray absorption and ATR-IR spectroscopy, Phys. Chem. Chem. Phys., 12 (2010) 5307-5316.
[27] T. Osako, K. Torii, Y. Uozumi, Aerobic flow oxidation of alcohols in water catalyzed by platinum nanoparticles dispersed in an amphiphilic polymer, RSC Advances, 5 (2015) 2647-2654.
[28] K. Heyns, H. Paulsen, Selective Catalytic Oxidation of Carbohydrates, Employing Platinum Catalysts, in: M.L. Wolfrom, R.S. Tipson (Eds.) Advances in Carbohydrate Chemistry, Academic Press1963, pp. 169-221.
[29] J.H.J. Kluytmans, A.P. Markusse, B.F.M. Kuster, G.B. Marin, J.C. Schouten, Engineering aspects of the aqueous noble metal catalysed alcohol oxidation, Catalysis Today, 57 (2000) 143-155.
[30] A.F. Lee, Mechanistic Studies of Alcohol Selective Oxidation, Heterogeneous Catalysts for Clean Technology, Wiley-VCH Verlag GmbH & Co. KGaA2013, pp. 11-38.
[31] D. Ferri, A. Baiker, Advances in Infrared Spectroscopy of Catalytic Solid–Liquid Interfaces: The Case of Selective Alcohol Oxidation, Top. Catal., 52 (2009) 1323-1333.
[32] L.J. Durndell, C.M. Parlett, N.S. Hondow, K. Wilson, A.F. Lee, Tunable Pt nanocatalysts for the aerobic selox of cinnamyl alcohol, Nanoscale, 5 (2013) 5412-5419.
[33] K. Kon, S.H. Siddiki, K.-i. Shimizu, Size-and support-dependent Pt nanocluster catalysis for oxidant-free dehydrogenation of alcohols, Journal of catalysis, 304 (2013) 63-71.
[34] M. Nicastro, L. Tonucci, N. d'Alessandro, M. Bressan, L.K. Dragani, A. Morvillo, Platinum tetrasulfophthalocyanine as selective catalyst for the aerobic oxidation of shikimic acid, Inorganic Chemistry Communications, 10 (2007) 1304-1306.
[35] A.F. Lee, K. Wilson, Structure-reactivity correlations in the selective aerobic oxidation of cinnamyl alcohol: in situ XAFS, Green Chem., 6 (2004) 37-42.
[36] A.F. Lee, C.V. Ellis, J.N. Naughton, M.A. Newton, C.M.A. Parlett, K. Wilson, Reaction-Driven Surface Restructuring and Selectivity Control in Allylic Alcohol Catalytic Aerobic Oxidation over Pd, Journal of the American Chemical Society, 133 (2011) 5724-5727.
[37] A.F. Lee, J.N. Naughton, Z. Liu, K. Wilson, High-Pressure XPS of Crotyl Alcohol Selective Oxidation over Metallic and Oxidized Pd(111), ACS Catalysis, 2 (2012) 2235-2241.
[38] S.F.J. Hackett, R.M. Brydson, M.H. Gass, I. Harvey, A.D. Newman, K. Wilson, A.F. Lee, High-Activity, Single-Site Mesoporous Pd/Al2O3 Catalysts for Selective Aerobic Oxidation of Allylic Alcohols, Angewandte Chemie International Edition, 46 (2007) 8593-8596.
[39] X. Han, L. Geng, Y. Guo, R. Jia, X. Liu, Y. Zhang, Y. Wang, Base-free aerobic oxidation of 5-hydroxymethylfurfural to 2,5-furandicarboxylic acid over a Pt/C-O-Mg catalyst, Green Chem., 18 (2016) 1597-1604.
[40] H. Ait Rass, N. Essayem, M. Besson, Selective aqueous phase oxidation of 5-hydroxymethylfurfural to 2,5-furandicarboxylic acid over Pt/C catalysts: influence of the base and effect of bismuth promotion, Green Chem., 15 (2013) 2240-2251.
[41] H. Ait Rass, N. Essayem, M. Besson, Selective Aerobic Oxidation of 5-HMF into 2,5-Furandicarboxylic Acid with Pt Catalysts Supported on TiO2- and ZrO2-Based Supports, ChemSusChem, 8 (2015) 1206-1217.
[42] H.P.L. Gemoets, Y. Su, M. Shang, V. Hessel, R. Luque, T. Noel, Liquid phase oxidation chemistry in continuous-flow microreactors, Chemical Society Reviews, 45 (2016) 83-117.
[43] B. Gutmann, U. Weigl, D.P. Cox, C.O. Kappe, Batch- and Continuous-Flow Aerobic Oxidation of 14-Hydroxy Opioids to 1,3-Oxazolidines—A Concise Synthesis of Noroxymorphone, Chemistry – A European Journal, 22 (2016) 10393-10398.

[44] D.S. Mannel, S.S. Stahl, T.W. Root, Continuous Flow Aerobic Alcohol Oxidation Reactions Using a Heterogeneous Ru(OH)x/Al2O3 Catalyst, Organic Process Research & Development, 18 (2014) 1503-1508.
[45] A. Gavriilidis, A. Constantinou, K. Hellgardt, K.K. Hii, G.J. Hutchings, G.L. Brett, S. Kuhn, S.P. Marsden, Aerobic oxidations in flow: opportunities for the fine chemicals and pharmaceuticals industries, Reaction Chemistry & Engineering, 1 (2016) 595-612.
[46] A. Muzen, M.S. Fraguío, M.C. Cassanello, M.A. Ayude, P.M. Haure, O.M. Martínez, Clean Oxidation of Alcohols in a Trickle-Bed Reactor with Liquid Flow Modulation, Industrial & Engineering Chemistry Research, 44 (2005) 5275-5284.
[47] L.J. Durndell, K. Wilson, A.F. Lee, Platinum-catalysed cinnamaldehyde hydrogenation in continuous flow, RSC Advances, 5 (2015) 80022-80026.
[48] T.-W. Kim, F. Kleitz, B. Paul, R. Ryoo, MCM-48-like large mesoporous silicas with tailored pore structure: facile synthesis domain in a ternary triblock copolymer− butanol− water system, Journal of the American Chemical Society, 127 (2005) 7601-7610.
[49] D. Zhao, J. Feng, Q. Huo, N. Melosh, G.H. Fredrickson, B.F. Chmelka, G.D. Stucky, Triblock copolymer syntheses of mesoporous silica with periodic 50 to 300 angstrom pores, science, 279 (1998) 548-552.
[50] J. Dhainaut, J.-P. Dacquin, A.F. Lee, K. Wilson, Hierarchical macroporous–mesoporous SBA-15 sulfonic acid catalysts for biodiesel synthesis, Green Chem., 12 (2010) 296-303.
[51] Christopher M.A. Parlett, Mark A. Isaacs, Simon K. Beaumont, Laura M. Bingham, Nicole S. Hondow, K. Wilson, Adam F. Lee, Spatially orthogonal chemical functionalization of a hierarchical pore network for catalytic cascade reactions, Nature Materials, 15 (2015) 178.
[52] L.J. Durndell, C.M. Parlett, N.S. Hondow, M.A. Isaacs, K. Wilson, A.F. Lee, Selectivity control in Pt-catalyzed cinnamaldehyde hydrogenation, Scientific reports, 5 (2015).
[53] S. Cameron, D. Dwyer, Surface core level shifts in Pt3Ti (111), Surface Science Letters, 176 (1986) L857-L862.
[54] G. Johansson, J. Hedman, A. Berndtsson, M. Klasson, R. Nilsson, Calibration of electron spectra, Journal of Electron Spectroscopy and Related Phenomena, 2 (1973) 295-317.
[55] C.M. Parlett, D.W. Bruce, N.S. Hondow, A.F. Lee, K. Wilson, Support-enhanced selective aerobic alcohol oxidation over Pd/mesoporous silicas, ACS Catalysis, 1 (2011) 636-640.
[56] C.M. Parlett, P. Keshwalla, S.G. Wainwright, D.W. Bruce, N.S. Hondow, K. Wilson, A.F. Lee, Hierarchically ordered nanoporous Pd/SBA-15 catalyst for the aerobic selective oxidation of sterically challenging allylic alcohols, ACS Catalysis, 3 (2013) 2122-2129.
[57] M.S. Ide, D.D. Falcone, R.J. Davis, On the deactivation of supported platinum catalysts for selective oxidation of alcohols, Journal of Catalysis, 311 (2014) 295-305.
[58] M. Caravati, J.-D. Grunwaldt, A. Baiker, Comparative in situ XAS investigations during aerobic oxidation of alcohols over ruthenium, platinum and palladium catalysts in supercritical CO 2, Catalysis Today, 126 (2007) 27-36.
[59] A.-B. Crozon, M. Besson, P. Gallezot, Oxidation of 9-decen-1-ol (rosalva) by air in aqueous media on platinum catalysts, New Journal of Chemistry, 22 (1998) 269-273.
[60] J. Beziat, M. Besson, P. Gallezot, Liquid phase oxidation of cyclohexanol to adipic acid with molecular oxygen on metal catalysts, Applied Catalysis A: General, 135 (1996) L7-L11.
[61] J.C. de Jesús, F. Zaera, Adsorption and thermal chemistry of acrolein and crotonaldehyde on Pt (111) surfaces, Surface science, 430 (1999) 99-115.
[62] J. Lee, B. Saha, D.G. Vlachos, Pt catalysts for efficient aerobic oxidation of glucose to glucaric acid in water, Green Chem., 18 (2016) 3815-3822.
[63] M.A. van Spronsen, J.W.M. Frenken, I.M.N. Groot, Observing the oxidation of platinum, Nature Communications, 8 (2017) 429.
[64] Q.-X. Cai, J.-G. Wang, Y.-G. Wang, D. Mei, Mechanistic insights into the structure-dependent selectivity of catalytic furfural conversion on platinum catalysts, AIChE Journal, 61 (2015) 3812-3824.
[65] C. Keresszegi, T. Mallat, J.-D. Grunwaldt, A. Baiker, A simple discrimination of the promoter effect in alcohol oxidation and dehydrogenation over platinum and palladium, Journal of Catalysis, 225 (2004) 138-146.

[66] L.K. Ono, B. Yuan, H. Heinrich, B.R. Cuenya, Formation and Thermal Stability of Platinum Oxides on Size-Selected Platinum Nanoparticles: Support Effects, The Journal of Physical Chemistry C, 114 (2010) 22119-22133.
[67] M.B. Mooiman, K.C. Sole, N. Dinham, The Precious Metals Industry, Metal Sustainability, John Wiley & Sons, Ltd2016, pp. 361-396.